

# Application of non-contact ultrasonic method in air to study fiber-cement corrugated boards

Radosław DRELICH<sup>\*</sup>, Michał ROSIAK, and Michał PAKUŁA

Faculty of Mechatronics, Kazimierz Wielki University, Kopernika 1, 85-074 Bydgoszcz, Poland

**Abstract.** The fiber-cement and cellulose boards are materials commonly used in architectural engineering for exterior and interior applications such as building facades or as wall and roof covering materials. The aim of the study was to present the ultrasonic non-contact method of testing fiber-cement boards with Lamb waves and to discuss the results and limitations of the method in context of quality control of the material. The experiments were performed for the corrugated boards using a laboratory non-contact ultrasonic scanner. Lamb waves were generated in the tested materials by a transmitter excited by a chirp signal with a linearly modulated frequency. Waves transmitted through the tested material are acquired by the receiver and registered by the PC based acquisition system. The tests were done on reference plate board and the corrugated boards. As the main descriptor to assess the quality of tested boards the maximum amplitude of transmitted Lamb waves was selected. The significant role of boundary effects and frequency of waves was noticed. The obtained results have confirmed the usefulness of the applied ultrasonic method for testing macroscopic inhomogeneity of corrugated fiber-cement boards.

**Key words:** Lamb wave; cellulose fiber cement boards; non-contact ultrasonic methods.

## 1. Introduction

Flat and corrugated board materials such as drywall, fiber-cement boards, plywood, plastic boards, polymer-fiber composites, etc. are widely used in construction, automotive, aerospace and other industries as structural, structural and decorative elements, roofing and others. As a standard, tests of such materials are performed using destructive methods and are focused on measuring mechanical parameters (bending strength tests), geometrical parameters, density, water or vapor permeability, defined by relevant standards (PN-EN 492:2013-03, PN-EN ISO 178:2019-06). The disadvantages of these methods include their selective and destructive nature and the fact that it is necessary to take test samples with relatively small dimensions compared to the total plate dimensions. Moreover, these methods do not allow for continuous (for each manufactured board) monitoring of the quality of the boards during or after production. These limitations can be eliminated, or their role can be significantly reduced by applying, in addition to the tests required by the standard, tests with the use of ultrasonic non-destructive methods, using techniques in contact [1–4], semi-contact [5–6] or without contact [7–17]; see also review articles [18–19].

In the study, the examination of corrugated boards was performed using the non-contact ultrasonic technique using Lamb waves, the effectiveness of which has been confirmed in the diagnostics of fiber-cement flat plates, [11]. This method uses leaky Lamb waves generated in and received from the test material from the air (airborne Lamb waves).

The advantages of this method in comparison with the contact methods [1–4] is that there is no need to use a coupling substance between the tested material and transducers (e.g., water or ultrasonic gel). This fact significantly simplifies the measurements, improves the repeatability of the obtained results. It is particularly important from the point of view of the automatization of the measurement procedure, which is essential during monitoring the boards quality in industrial conditions (e.g., in motion on the production line).

This is of particular importance in the application of this measuring technique to test porous board materials, hygroscopic drywall, fiber-cement boards or plywood. If such materials were tested by conventional (contact) ultrasound techniques, the measurement would require the use of couplers that penetrate the material causing non-stationarity of the signals and leading to false results. The advantage of non-contact techniques, resulting from the lack of the need to use coupling substances, is the technical simplicity of implementation of the repetitive transmission of waves to and from the material, which makes it possible to perform a quick scan of the boards not only in the case of flat but also in the case of curved surfaces of the tested elements. This may apply to objects such as elements of aircraft covers, elements of building structures, or corrugated boards used mainly for roofing. The listed advantages of the non-contact technique may be the reason for their use in the quality control of construction boards at the stage of their production or after its completion.

The aim of the study is to present the ultrasonic non-contact (airborne) method of testing fiber-cement boards with Lamb waves and to discuss the results and limitations of the method, important from the point of view of effective use of the proposed technique for diagnostics of these materials. Novelty of the studies presented in the manuscript results from the fact that

\*e-mail: radeko@ukw.edu.pl

Manuscript submitted 2020-10-15, revised 2021-02-01, initially accepted for publication 2021-03-03, published in April 2021

to the knowledge of authors there are no studies on ultrasonic tests of corrugated boards in the literature. There are investigations concerning theoretical and experimental studies of the flat boards having periodically corrugated surfaces, [20]. However, in that case only the top and bottom surfaces of the sheets are irregular, while the core of the board is flat.

## 2. Model, materials, experimental setup

Assuming that the wavelengths used are much shorter than the pitch of corrugation profile (in the case of fiber-cement corrugated boards, the wavelength of the Lamb wave for the center frequency of the 50 kHz transducer is approx. 25 mm, while the pitch of corrugation profile is 130 mm) we assume that the Lamb wave propagation model in flat plates is in force.

The materials tested are the reference flat homogeneous polymer plate and the commercially available fiber-cement corrugated boards used mainly for roofing systems.

**2.1. Fundamentals of Lamb wave.** Lamb waves belong to the group of so-called guided waves and can propagate in materials limited between two parallel surfaces (e.g., in plates or shells) whose distance is comparable to the wavelength. They are the result of the simultaneous occurrence of longitudinal waves in the plate and transversely polarized waves (the direction of the particle movement perpendicular to the plate surface), [20]. The waves arise as a result of multiple reflections of the mentioned types of waves from the surfaces of the plate and their amplification and attenuation. Lamb waves are multi-mode in nature, and their propagation manifests itself in the form of two types of modes: symmetric and antisymmetric. The symmetric modes are termed the extensional modes because the average

displacement over the thickness is in the longitudinal direction. For the antisymmetric modes, the average displacement is in the transverse direction, and these modes are generally termed the flexural modes. For low frequencies two basic modes (symmetric mode S0 and antisymmetric mode A0) propagate, while as the frequency increases, the number of modes that can occur simultaneously in the plate increases (generally to infinity). The parameters of the Lamb waves strongly depend on the frequency and their frequency characteristics are called dispersion curves. For a homogeneous isotropic plate with a thickness  $h = 2d$ , these curves are determined on the basis of the Rayleigh-Lamb equations [21]:

- for symmetric modes (S)

$$\frac{\tan(qh)}{\tan(ph)} = \frac{-4k^2 pq}{(q^2 - k^2)^2}, \quad (1)$$

- for antisymmetric modes (A)

$$\frac{\tan(qh)}{\tan(ph)} = \frac{-(q^2 - k^2)^2}{4k^2 pq}, \quad (2)$$

where  $p$  and  $q$  are given by relationships

$$q^2 = \left( \frac{\omega^2}{c_T^2} - k^2 \right), \quad p^2 = \left( \frac{\omega^2}{c_L^2} - k^2 \right), \quad k = \frac{\omega}{c_p},$$

$k$  denotes the wavenumber,  $c_L$ ,  $c_T$  are the velocities of longitudinal and shear waves in the plate material, and  $c_p$ ,  $\omega = 2\pi f$  are the phase velocity and circular frequency of the Lamb wave, respectively. Figure 1 presents exemplary dispersion curves calculated based on Eqs. (1) and (2) for homogeneous plate of thickness  $h = 8.5$  mm for frequencies  $f = 20$ –120 kHz. The

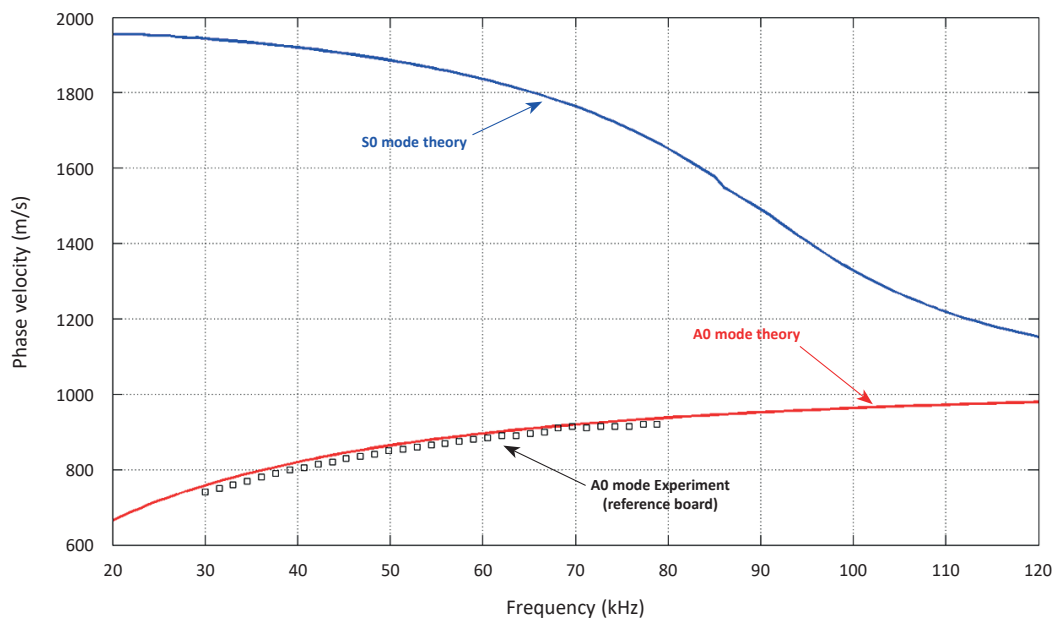


Fig. 1. Phase velocity of Lamb waves. Predictions of theoretical model (“—” and “—”) vs experimental results (□) obtained for reference board – Ertalon® 6 SA

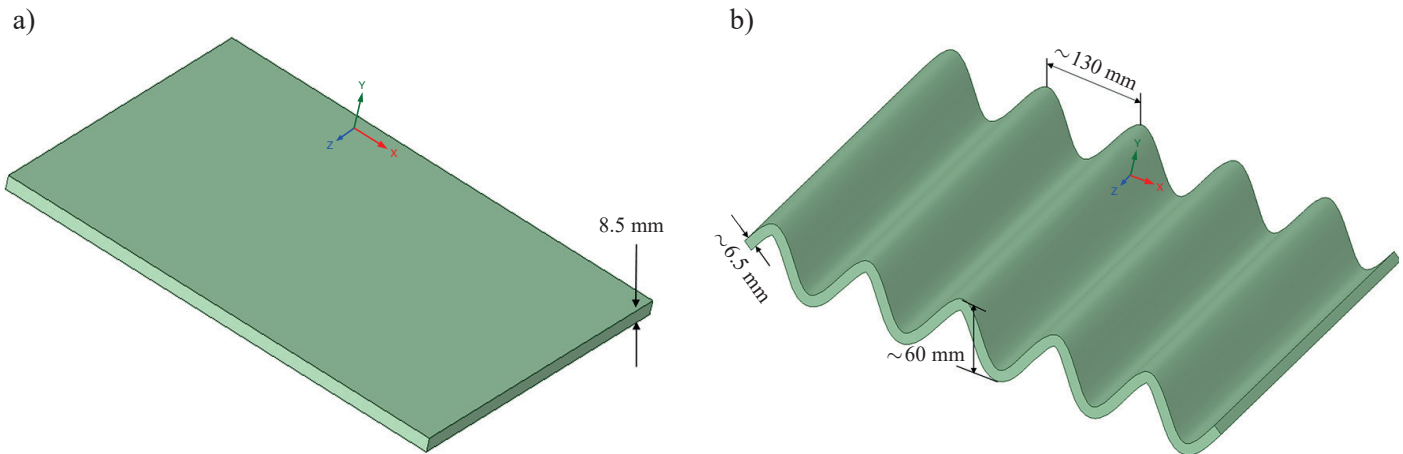


Fig. 2. Schematic picture of geometrical parameters of flat (a) and corrugated (b) boards

frequency range corresponds to the range used in the experimental studies discussed in the further sections of the paper. The calculations for model predictions were performed for a reference polymer plate and the input parameters are presented in Table 1.

Table 1  
Input parameters for calculations of dispersion curves  
for reference board – Ertalon® 6 SA

Input parameter	Value
Board Thickness	8.5 mm
Density	1.14 g/cm <sup>3</sup>
Velocity of longitudinal wave $c_L$	2656 m/s
Velocity of shear wave $c_T$	1048 m/s
Frequency range	20–120 kHz

It can be seen that the two basic Lamb wave modes, – symmetric  $S_0$  and antisymmetric  $A_0$ , are observed in the analyzed frequency range. The theoretical predictions of the model were compared with the phase velocity measured in the reference plate performed within independent experiments (see Fig. 1) using an automatic ultrasonic device for non-contact testing of surface waves or plate waves, [22, 23].

The non-contact ultrasonic technique presented in [22] uses a method in which the transmitter remains stationary while the receiving transducer moves away with a given step. In the case of studies presented in the paper the spatial step was 5 mm, the initial distance between emitter and receiver was 100 mm, while the final distance was 300 mm, so the total measurements distance was 200 mm. Recorded at each step signals, are processed using the Slant-Stack algorithm, which allows to determine the phase velocity as a function of frequency (see Fig. 1), [24]. It can be seen that the measured wave velocity as a function of frequency (black squares) is close to the theoretical predictions for the basic antisymmetric mode  $A_0$  (red line). It proves that in the ultrasonic experiments presented in the paper, the

measured signals are associated with propagation of the  $A_0$  antisymmetric mode.

**2.2. Materials.** The reference material are flat plates made of plastic (polyamide PA6) available on the market under the trade name Ertalon® 6SA with dimensions of  $8.5 \times 1000 \times 1230$  mm. These boards are obtained by the extrusion method, thanks to which they are characterized by homogeneity and the absence of internal defects. It was the main reason for considering them as reference material. The tested corrugated boards are commercially available fiber-cement construction boards with dimensions of  $6.5 \pm 0.6 \times 1150 + 5/-10 \times 1250 \pm 10$  mm and a profile dimension of 130 mm (see Fig. 2), with a moisture content of approx. 2% (the boards were seasoned in laboratory conditions of approximately 3 months).

The corrugated fiber-cement boards are made as a mixture of Portland cement (CEM I + II 71 – 83.2%), with the addition of inert fillers (lime, mica, silica 10%), cellulose fibers (3–5%), polyvinyl alcohol (1.8–2%) and pozzolanic filler – cenospheres from fly ash 0–6%). Polyvinyl alcohol fibers are added to increase the strength, flexibility, and durability of the boards. In the production process, these boards undergo a process of forming, maturing, and drying so manufacturing defects may occur at any stage. These materials, due to their multi-component contents, may be characterized by a certain heterogeneity in structure, density (manufacturer indicate a minimum density of  $1400 \text{ kg/m}^3$ ) or mechanical properties. Fiber-cement boards have good sound absorption, resistance to chemical factors (the external surfaces can be painted or additionally protected with e.g., wax to reduce water absorption), they are good thermal insulators and are non-flammable.

The most common fiber-cement products are flat plates with a smooth surface or with a texture and corrugated plates. The latter are mostly used for roofing in farm buildings, industrial buildings or even including residential buildings.

**2.3. Experimental setup.** The idea of the elaborated measurement method used for corrugated or flat plate materials and photography of a laboratory scanner during the measurements

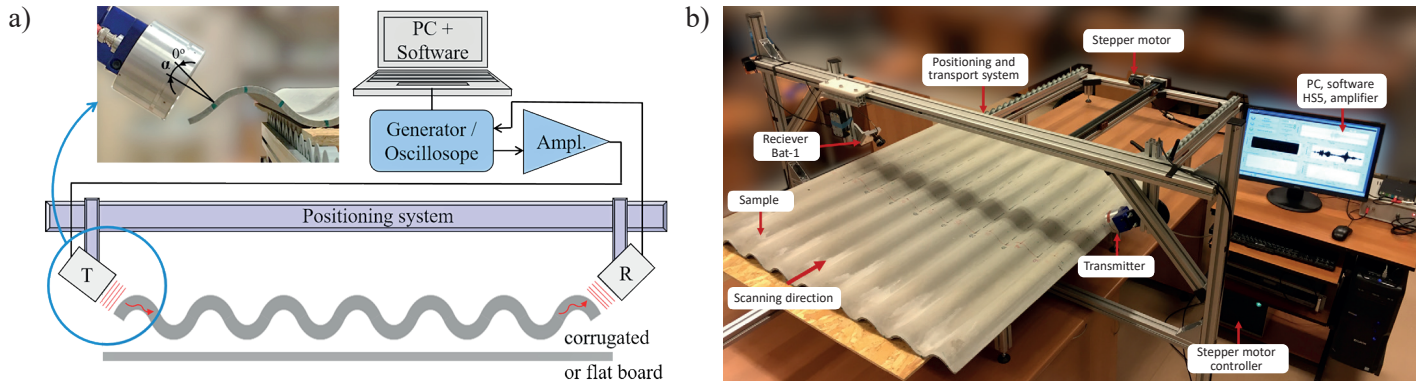


Fig. 3. Scheme of experimental setup for airborne ultrasonic studies of boards using Lamb waves (a) and photography of non-contact ultrasonic scanner during experiments for corrugated boards (b)

is shown in Fig. 3. This multifunctional device allows testing plate materials with a maximum size of  $1550 \times 1600$  mm using the plate waves, surface waves, and longitudinal waves.

The applied method uses Lamb waves, which in the case of corrugated boards propagate perpendicular to the direction of the profile of the board. These waves are generated in the material using the longitudinal wave incident from the air, excited by the transmitter (T), placed a few centimeters from the tested plate. The transmitter, placed close to the edge of the board, is inclined to its surface at a critical angle  $\alpha_c$  [21]. Lamb waves excited in the board (according to the model presented in Section 2.1 it can be observed many of them) propagate in the material, and part of their energy leaks to the air. The receiver (R) located on the opposite edge of the plate (vis-a-vis of the transmitter and also inclined to the plate surface at a critical angle) allows to acquire leaked waves from the air. The theoretical critical angles ( $\alpha_c$ ) for individual materials (reference and corrugated boards) are determined based on Snell's law [7]:

$$\alpha_c = \arcsin\left(\frac{c_L^{air}}{c_{Lamb}^{plate}}\right), \quad (3)$$

where  $c_L^{air}$  is the velocity of longitudinal wave in air, while  $c_{Lamb}^{plate}$  is the Lamb wave velocity in board material. The Lamb's wave velocity is not known in advance. Thus, it was evaluated theoretically based on dispersion relation from Eqs. (1) and (2). The applications of these relationships require to determine the velocities of shear and longitudinal waves in the board material. They were measured using the contact ultrasonic transmission method, and their values are listed in Table 2. The experiments to determine the shear and longitudinal wave velocity were performed using a pair of shear (V101-RM) and longitudinal (V318-SU) wave transducers (PANAMETRICS®) excited by pulse signal generator 5058PR (PANAMETRICS®).

Finally, the values of the theoretical phase velocity of A0 Lamb wave were used to calculate the initial value of critical angle. Then to find an optimum critical angle (for a given frequency) transmitter and receiver were varied slightly around the calculated initial value and the amplitude of the received signal

observed as criteria for optimal value of critical angle. The identified critical angles for reference and corrugated fiber-cement boards are  $(20^\circ)$  and  $(14^\circ)$ , respectively.

Table 2  
Input parameters for calculations of  $\alpha_c$

Input parameter	Value
Velocity of longitudinal wave $c_L^{air}$ in air	345 m/s
Velocity of shear wave $c_T^{plate}$ in corrugated plate	1572 m/s
Velocity of longitudinal wave $c_L^{plate}$ in corrugated plate	2741 m/s

The scanner consists of a manual head positioning system, a transport system for moving the tested plates, which uses a drylin® (Igus®) rope drive driven by a hybrid servo drive (Easy-Servo), a servo drive control system, two ultrasonic transducers: a signal transmitter and receiver, a generator arbitrary signals with the two-channel Handyscope HS5 oscilloscope, a custom-made wideband (10 kHz – 1.8 MHz) power amplifier (gain 75 dB) and a computer with software for controlling the sample movement, measurement data acquisition and signal analysis.

As emitters were used non-contact ultrasonic transducers called gas Matrix Piezoceramics (The Ultrason Group®) characterized by center frequencies of 30, 50, and 100 kHz and active diameters of approx. 60 mm. A broadband membrane receiver type Bat-1 (Microacoustics®) with an active surface of approx. 10 mm was used as the receiving transducer.

The transmitters were excited using chirp signals of linearly variable frequency. For each of them the optimal frequency ranges of the chirp signal were selected experimentally, i.e., the minimum frequency  $f_{min}$  and the maximum  $f_{max}$ , taking into account the maximization of the Lamb wave energy and the favorable signal-to-noise ratio. The applied frequency ranges of emitted signals are shown in Table 3. The time duration/excitation of the transmitter for all cases was 300 ms, while the acquisition time was 310 ms. The results for the reference material were obtained in the frequency range from 20 kHz to

Table 3

Chirp frequency ranges used to excite emitters having center frequencies of 30, 50, and 100 kHz

Material	Central frequency of transmitter and selected frequency range of chirp signal		
	30 kHz $f_{min} - f_{max}$	50 kHz $f_{min} - f_{max}$	100 kHz $f_{min} - f_{max}$
Ertalon® 6 SA	21–38 kHz	42–72 kHz	–
Corrugated board	21–38 kHz	35–72 kHz	87–110 kHz

70 kHz. The signals from the transducer of center frequency 100 kHz had a low signal-to-noise ratio resulting from significant attenuation of these waves in the polymer. Results of the wave propagation for the corrugated boards were measured over a wider frequency range from 20 kHz to 110 kHz and were obtained using transmitters with main frequencies of 30, 50, and 100 kHz.

The scanner shown in Fig. 3b along with the custom-made software allows for the movement of the tested boards against immobile ultrasonic transducers with a minimum spatial step of 1 mm and recording of signals for individual measurement points. In the present paper, the measurements of the reference board were made with a spatial step 2 mm (656 measurement points), while for corrugated plates, the signals were recorded with a spatial step 3 mm (437 measurement points). The software for control of the scanner allows setting the frequency range and amplitude of the generated signals, the gain of received signals, the selection of the time window, and the use of averaging signals in the time domain to reduce noise.

**2.4. Signal processing.** The main parameter used in the analysis was the maximum value of the amplitude as a function of the position in the plate. In order to minimize the impact of air fluctuations (movement of air particles and local changes of its parameters) on the recorded signals, the measured amplitudes were smoothed using the moving average method, taking 3 points for averaging.

Figure 4 shows the successive stages of the signal processing procedure, based on the example of a measurement made for a fiber-cement corrugated board using a transducer with a main frequency of 50 kHz.

In the first step, the Lamb wave signal recorded in a given position of the plate, from the receiving transducer, is correlated with the pattern signal, and an exemplary result of this correlation in the form of the so-called A scan is shown in Fig. 4a. In the middle part of this time window (between 1 and 1.1 ms), it is visible the main pulse of the Lamb wave mode A0 with a maximum amplitude of about 35 V. The remaining signal components, visible in the A-scan, have a much smaller amplitude and are not included in further analysis. The signals shown on the A-scan, recorded for all measuring points (for the entire plate), are shown in Fig. 4b in the form known from ultrasound imaging as B-scan. Next to the B-scan is a grayscale color map showing what color of the image corresponds to the amplitude of the measured signal.

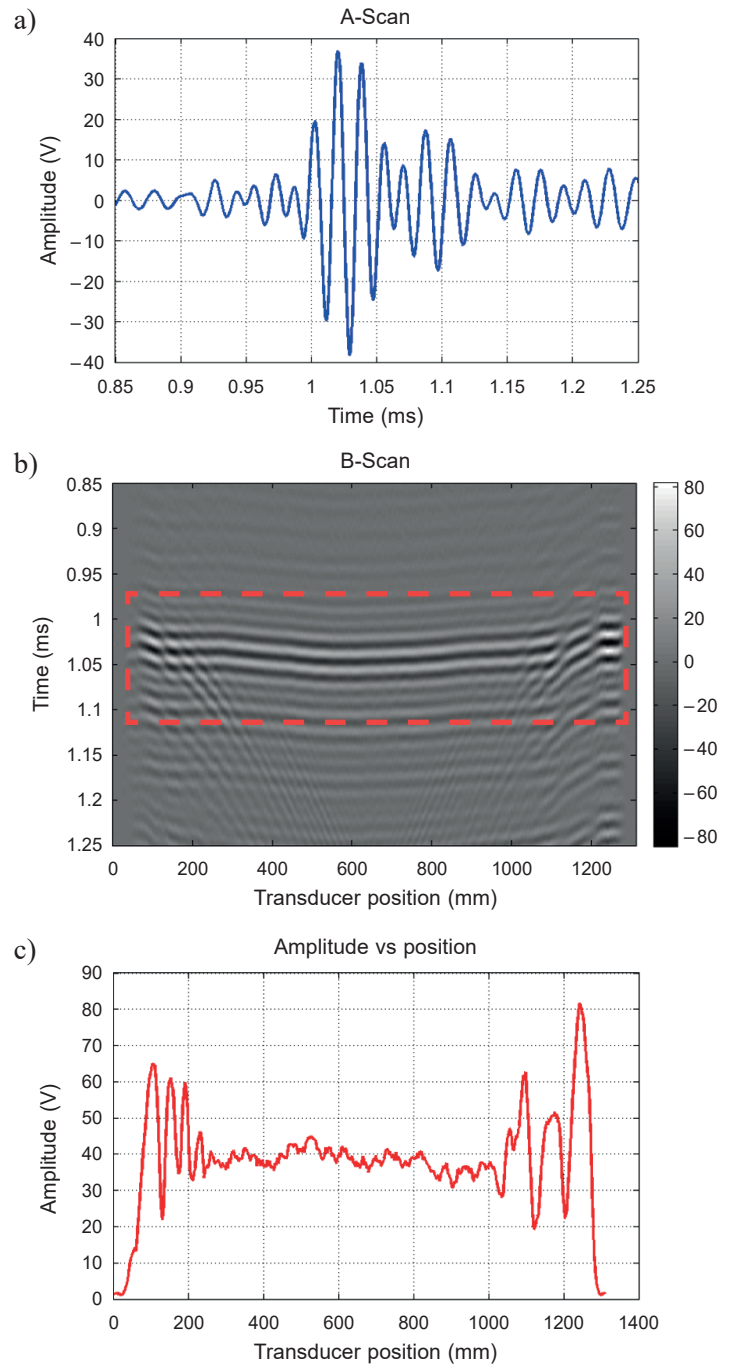


Fig. 4. Three steps of signal analysis: A-Scan (a), B-scan (b), and maximum amplitude vs position (c)

The B-scan allows for a qualitative analysis of wave propagation in the plate, in particular from the point of view of the variability of wave velocity and amplitude as well as interaction of the wave with board boundary. Further analysis of the obtained results is performed for part of the signals inside the window marked with a red dotted line (see Fig 4b). It can be seen that near the plate border (@ ~ 50 mm and @ ~ 130 mm position) the ultrasound image is not continuous, which suggests that in this area the recorded signals contain many interfering wave components. Yet another factor that hampers inter-

pretation of ultrasonic experiments may result from imperfect shape of the manufactured corrugated boards (manufacturer states tolerances for each dimensions  $\pm 0.6$  mm for thickness,  $\pm 10$  mm in length, and  $+5/-10$  mm in width). It is particularly noticeable in the B-scan, where parabolic “shape” of the time of flight of signals as a function of position is shown (see Fig. 4b). TOF is the sum of time of wave propagation in the board and in air (between transducers and the board). While in the case of reference board, having well defined regular dimensions, distance between transducers and the board is constant (scan B Fig. 5a), then in the case of corrugated boards, because of the imperfect shape, this distance in air between board and transducers may change and it may influence the obtained results.

In the last stage of signal processing, the maximum amplitude of the Lamb wave pulse is determined and plotted as a function of the position (see Fig. 4c). Image discontinuity due to interfering wave components near the edge of the plate, seen in scan B, is also reflected in the maximum amplitude oscillation. The geometrical imperfections of corrugated boards, which generate the parabolic “shape” of the time of flight seems not to influence the wave amplitude. Such behavior can be explained by low attenuation of waves in air (about 1 dB/m @50 kHz) in comparison with the material of boards (about 50 dB/m @50 kHz). Another possibility is that the effect could be hidden in fluctuations of wave amplitudes.

### 3. Results and Discussion

The section presents the results of Lamb wave propagation measurements carried out for a flat and homogeneous polymer board (Ertalon® 6SA), considered as reference material, and the results obtained for corrugated fiber-cement plates.

**3.1. Reference material.** The results for the reference material were obtained using two ultrasonic transducers with the main frequencies of 30 and 50 kHz. According to the description of the method (especially regarding the interpretation of signal processing results – see Chapter 2.4), the attention will be focused on the basic antisymmetric mode (A0), which is the main wave energy carrier in the tested plates. Confirmation that the measured signal is the antisymmetric mode (A0) was obtained by independent measurements of the Lamb wave dispersion both in the reference material and in the tested corrugated plates along the corrugations, compared to the results of theoretical predictions (see Sec. 2.1). The results of measurements of Lamb wave propagation for the reference material obtained with the use of a transducer with a center frequency of 30 kHz are shown in Fig. 5. The B-scan presented in Fig. 5a shows that two qualitatively different areas can be distinguished: (i) the boundary area (at the beginning and at the end of the scanned plate) in which there is interference of the traveling wave with the waves reflected from the edge, and (ii) the central area, where the amplitudes of the wave pulses are parallel to the position axis which proves that the wave velocity is approximately constant.

The boundary areas cover a distance of approx. 230 mm of the slab from the edges, while the central part of the plate

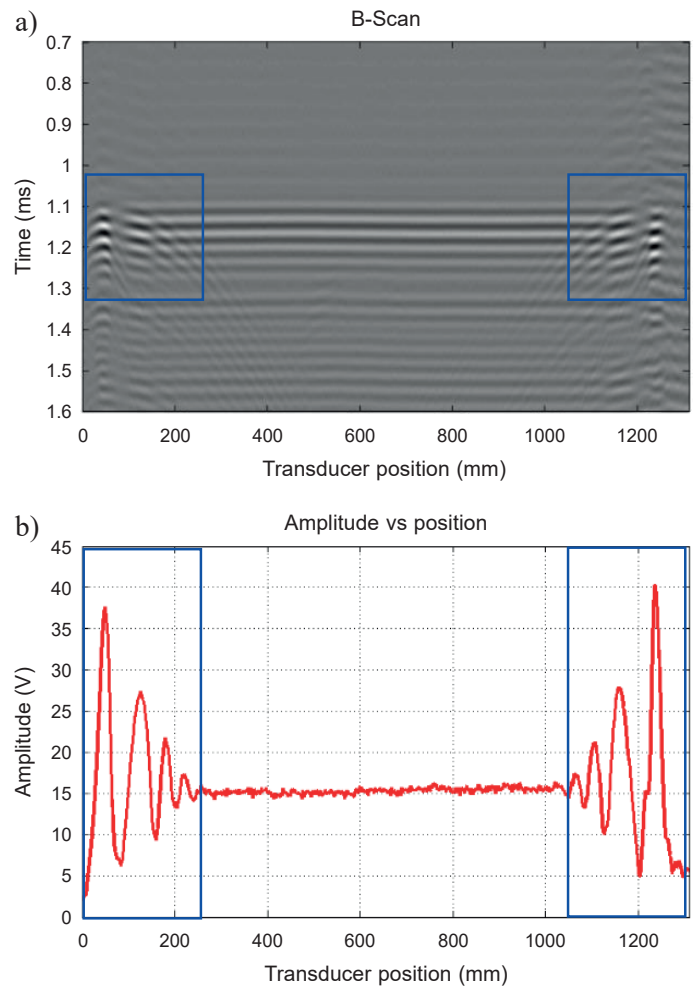


Fig. 5. B-scan (a) and maximum amplitude vs position (b) for reference material measured 30 kHz, blue windows shows the boundary areas

is approx. 770 mm long (from approx. 230 to 1020 mm). The same two areas are shown in the graph of the normalized maximum amplitude versus the mean maximum amplitude from the central region as a function of position, shown in Fig. 5b, which illustrates the presence of strong oscillations of the maximum amplitude of the signal at the boundaries of the plate (marked ranges) and an approximately constant amplitude in the central part of the chart.

The constant wave velocity and amplitude prove that the material is homogeneous. It is worth adding that the presence of these two areas was observed both in the reference material and in all tested corrugated boards.

**3.2. Corrugated board.** The experimental results for corrugated boards were divided into two groups. First, the relationship of the maximum amplitude of the Lamb wave as a function of position for one plate was compared with the use of three main frequencies (30, 50 and 100 kHz). Then the normalized amplitude for five corrugated plates of the same type was compared with using the above-mentioned three measuring frequencies.

A comparison of the maximum amplitudes for the same plate tested using Lamb waves of different main frequencies,

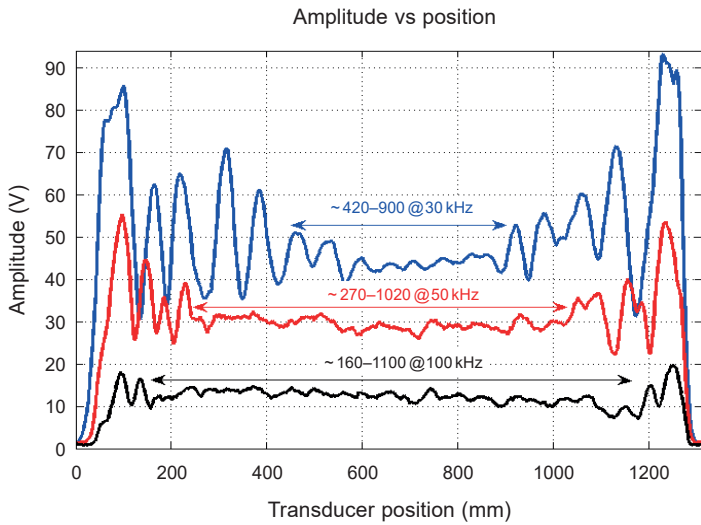


Fig. 6. Maximum amplitudes of Lamb waves measured @ 30, 50, 100 kHz vs position with marked by arrows ranges of approximately constant values amplitudes

see Fig. 6, shows that the mean amplitude and the range of the boundary area decrease with increasing frequency. The ranges of areas that can be classified as central, where the wave interference is not dominant, for the frequencies of 30, 50 and 100 kHz, are, respectively, approx. 480 mm (from 420 to 900 mm), approx. 750 mm (from 270 to 1020 mm) and approx. 940 mm (from 160 to 1100 mm).

For the given frequency, the amplitude oscillations in the boundary regions are similar but not fully symmetrical (at the beginning they have a slightly different trend than at the end). Comparing the mentioned results for the corrugated boards with the result for the reference plate board (see Fig. 5a) where this symmetry is more pronounced, suggest that the material properties of the corrugated boards in the boundary region are heterogeneous.

The heterogeneity of the plate properties is also evident in the central region where both oscillations and changes in the amplitude trend occur. It can be concluded that the use of higher ultrasonic frequencies for testing fiber-cement boards, limits the measuring range in which the edge interference effects are observed, thus increasing the area of relative amplitude stabilization. One can notice that in the measuring range where there are strong amplitude oscillations, the diagnostic possibilities of the Lamb wave method are limited, because the potential occurrence of defects in this area of the tested plate may be obscured by strong signal oscillations resulting from edge effects.

In order to compare the results of the Lamb wave test for a larger number of corrugated plates, the results of the normalized maximum amplitude (relative to the mean of the central area about 400 mm long) as a function of position for five plates of the same type, are collected in the graphs shown in Fig. 7. The values of the average maximum amplitudes from the central area of the plates, used in the normalization, are about 50, 30, and 10 V, respectively for the frequencies of 30, 50, and 100 kHz. For a single plate, these differences are visible

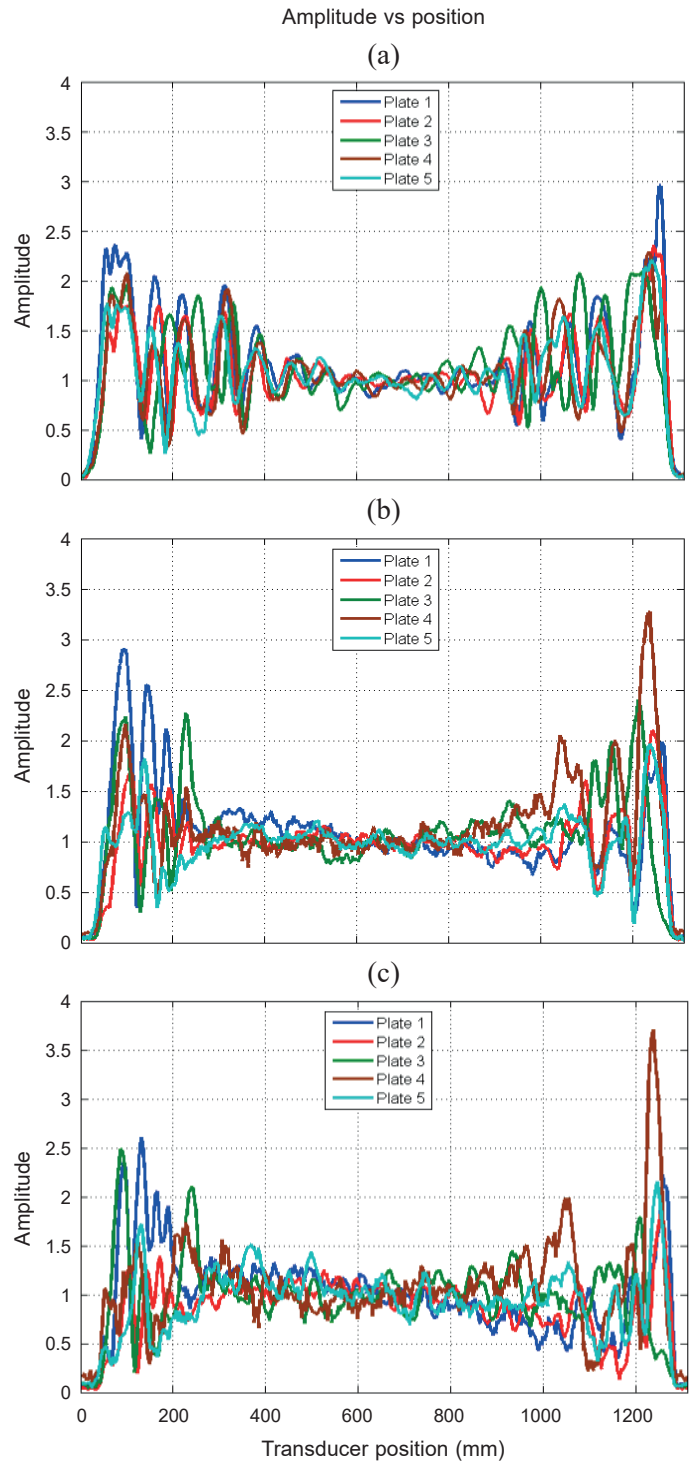


Fig. 7. Comparison of amplitudes of lamb waves vs position measured @30, 50, 100 kHz for 5 corrugated fiber-cement boards

in Fig. 6. The standard deviations of the maximum amplitude determined for the 5 plates were approximately 10, 10, and 5 V, respectively.

It is worth noting that the previously observed regularities for one plate, regarding the occurrence and extent of the boundary area for individual frequencies, are confirmed for all plates. At the same time, it is visible that the amplitude

differences related to the heterogeneity of the properties of individual plates are more visible in the boundary area than in the middle area.

There is also a clear asymmetry of oscillations in the boundary regions, which indicates that the non-homogeneity at the boundary is not of a similar nature, i.e., they are different for each plate. A comparison of the normalized wave's amplitude for different frequencies of the measuring transducers shows that the noise level in relation to the signal amplitude at the edge is rather independent of the frequency used. This may indicate that the noise is not caused by scattering on inhomogeneities, which are a function of wavelength.

**3.3. Reference vs. Corrugated.** To better understand the Lamb wave's amplitude variation component in the corrugated plates, related to the material inhomogeneity, Fig. 8 compares the normalized amplitude results for the selected corrugated plate and the reference plate for the 30 kHz main frequency. Throughout the scanning area, greater amplitude changes are observed for the corrugated plate than for a homogeneous polymer plate. This indicates that the material origin of the amplitude changes both in the boundary region and beyond. Moreover, taking into account the fact that the wave signals are obtained along the entire length of the plates, transversely to the undulations, in the frequency range from 20 to 110 kHz, the results obtained in the study prove that the proposed non-contact Lamb wave method can be used for non-destructive testing of fiber-cement plates.

authors of the study did not find similar results in the literature relating to the testing of other construction materials (e.g., metal plates, composites, glued joints) using the Lamb wave method. In order to take into account the influence of undulations of the tested fiber-cement boards and their material inhomogeneities on Lamb waves, further research is needed, including the use of advanced modeling, the basis of which can be found e.g., in [25–27].

## 4. Conclusions

The results of the conducted measurements show that the proposed non-contact ultrasonic technique allows to observe the propagation of Lamb waves in fiber-cement corrugated boards in a wide frequency range from about 20 to 110 kHz. The analysis of the properties of the measured waves shows that the main antisymmetric (A0) mode is observed, which propagates along the entire plate (approx. 1 m long), transversely to the undulations. The ultrasonic images (B scans) show strong boundary effects in the form of oscillation of the wave's amplitude. Moreover, it is also noticeable parabolic “shape” of the time of flight of signals as a function of position being result of imperfect shape of the manufactured corrugated boards. This effect was not observed for the wave amplitudes and thus, this parameter was preferred in the analysis.

In the case of using a simple diagnostic criterion in the form of the transmitted wave's amplitude value, the boundary effects can significantly limit the area of plate diagnosis. Therefore, it seems that for diagnostic purposes in the boundary zone there is a need to develop a more advanced method of interpreting signals from this region. The obtained results also show that the boundary effect range increases for longer (lower frequency) waves. It is worth paying attention to the fact that amplitude fluctuations are observed throughout the scanning area, which is especially visible in fiber-cement boards. Comparing the results for the corrugated boards with the results for a homogeneous polymer board indicates the material origin of the fluctuations.

In further works on the use of the method, it is worth focusing on determining the causes of the observed amplitude fluctuations, the type of material inhomogeneities that causes them, and the role of humidity.

A separate issue is the problem of diagnostic efficiency assessment for defect detection and finding defect descriptors in boundary areas. In the field of experimental research, there is a need to develop a measurement technique in order to suppress unwanted signals coming from wave reflections, from the elements of the measuring system.

## REFERENCES

- [1] Z. Su, L. Ye, and Y. Lu, “Guided Lamb waves for identification of damage in composite structures: A review”, *J. Sound Vibr.* 295, 753–780 (2006).
- [2] J.K. Agrahari and S. Kapuria, “Effects of adhesive, host plate, transducer and excitation parameters on time reversibility of ultrasonic Lamb waves”, *Ultrasonics* 70, 147–157 (2016).

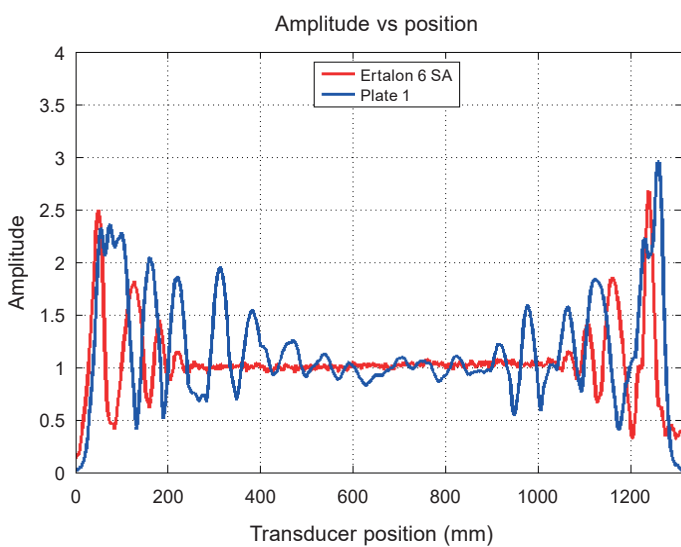


Fig. 8. Comparison of normalized amplitudes of Lamb waves vs position measured @30 kHz for reference boards (Ertalon 6 SA) and selected corrugated board

Earlier reports in the literature on fiber-cement materials and the non-contact method were limited to flat plates and frequencies around 100 kHz [11]. At that time, there was no clear justification for differentiating the results in the boundary area and the central area in the plate, and it was not possible to assess the extent of individual areas depending on the frequency. The



Application of non-contact ultrasonic method in air to study fiber-cement corrugated boards

- [3] R. Kędra and M. Rucka, "Preload monitoring in a bolted joint using Lamb wave energy", *Bull. Pol. Acad. Sci. Tech. Sci.* 67(6), 1161–1169 (2019).
- [4] S. Vázquez, J. Gosálbez, I. Bosch, A. Carrión, C. Gallardo, and J. Payá, "Comparative Study of Coupling Techniques in Lamb Wave Testing of Metallic and Cementitious Plates", *Sensors (Basel)* 19(19), 4068 (2019).
- [5] L. Yu, Z. Tian, and C.A.C. Leckey, "Crack imaging and quantification in aluminum plates with guided wave wavenumber analysis methods", *Ultrasonics* 62, 203–212 (2015).
- [6] M. Radziński, P. Kudela, W. Ostachowicz, P. Bolimowski, R. Kozera, and A. Boczkowska, "Lamb-wave-based method in the evaluation of self-healing efficiency", *Appl. Sci.* 10, 2585 (2020).
- [7] K. Imielińska, M. Castaing, R. Wojtyrab, J. Harasa, E. Le Clezio, and B. Hosten, "Air-coupled ultrasonic C-scan technique in impact response testing of carbon fibre and hybrid: glass, carbon and Kevlar/epoxy composites", *J. Mat. Process. Techn.* 157–158, 513–522 (2004).
- [8] H.B. Kichou, J.A. Chavez, A. Turo, J. Salazar, and M.J. Garcia-Hernandez, "Lamb waves beam deviation due to small inclination of the test structure in air-coupled ultrasonic NDT", *Ultrasonics* 44, e1077–e1082 (2006).
- [9] S. Yashiro, J. Takatsubo, and N. Toyama, "An NDT technique for composite structures using visualized Lamb-wave propagation", *Compos. Sci. Technol.* 67, 3202–3208 (2007).
- [10] Ł. Ambrozinski, B. Piwakowski, T. Stepinski, and T. Uhl, "Application of air-coupled ultrasonic transducers for damage assessment of composite panels", *6th European Workshop on Structural Health Monitoring*, 2014, pp. 1–8.
- [11] R. Drelich, T. Gorzelańczyk, M. Pakuła, and K. Schabowicz, "Automated control of cellulose fibre cement boards with a non-contact ultrasound scanner", *Autom. Constr.* 57, 55–63 (2015).
- [12] M.S. Harb and F.G. Yuan, "Non-contact ultrasonic technique for Lamb wave characterization in composite plates", *Ultrasonics* 64, 162–169 (2016).
- [13] S. Talberg and T.F. Johansen, "Acoustic measurements above a plate carrying Lamb waves", *Proceedings of the 39th Scandinavian Symposium on Physical Acoustics*, Geilo, Norway, 2016.
- [14] T. Marhenke, J. Neuenschwander, R. Furrer, J. Twiefel, J. Hasener, P. Niemz, and S.J. Sanabria, "Modeling of delamination detection utilizing air-coupled ultrasound in wood-based composites", *NDT E Int.* 99, 1–12 (2018).
- [15] K.J. Vössing, M. Gaal, and E. Niederleithinger, "Air-coupled ferroelectric ultrasonic transducers for nondestructive testing of wood-based materials", *Wood Sci. Technol.* 6, 1527–1538 (2018).
- [16] N. Toyama, J. Ye, W. Kokuyama, and S. Yashiro, "Non-contact ultrasonic inspection of impact damage in composite laminates by visualization of lamb wave propagation", *Appl. Sci.* 9, 46 (2019).
- [17] A. Römmeler, P. Zolliker, J. Neuenschwander, V. van Gemmeren, M. Weder, and J. Dual, "Air coupled ultrasonic inspection with Lamb waves in plates showing mode conversion", *Ultrasonic* 100, 105984 (2020).
- [18] M. Kaczmarek, B. Piwakowski, and R. Drelich, "Noncontact ultrasonic nondestructive techniques: state of the art and their use in civil engineering", *J. Infrastruct. Syst.* 23(1), 45–56a (2017).
- [19] B. Yilmaz, A. Asokkumar, E. Jasiuniene, and R. J. Kazys, "Air-coupled, contact, and immersion ultrasonic non-destructive testing: Comparison for bonding quality evaluation", *Appl. Sci.* 10, 6757 (2020).
- [20] J. Liu and N.F. Declerq, "Ultrasonic geometrical characterization of periodically corrugated surfaces", *Ultrasonics* 53, 853–861 (2013).
- [21] J.D. Achenbach, *Wave propagation in elastic solids*, North-Holland Publishing Company, Amsterdam, 1973.
- [22] O. Abraham, B. Piwakowski, G. Villain, and O. Durand, "Non-contact, automated surface wave measurements for the mechanical characterization of concrete", *Constr. Build. Mater.* 37, 904–915 (2012).
- [23] R. Drelich, B. Piwakowski, and M. Kaczmarek, "Identification of inhomogeneous cover layer by non-contact ultrasonic method – studies for model materials", *Annales du Bâtiment et des Travaux Publics* 66(1–3), 47–52 (2014).
- [24] Ł. Amboziński, B. Piwakowski, T. Stepinski, and T. Uhl, "Evaluation of dispersion characteristics of multimodal guided waves using slant stack transform", *NDT E Int.* 68, 88–97 (2014).
- [25] W. Ke, M. Castaing, and C. Bacon, "3D finite element simulations of an air-coupled ultrasonic NDT system", *NDT E Int.* 42, 524–533 (2009).
- [26] A. Piekarczyk, "Test-supported numerical analysis for evaluation of the load capacity of thin-walled corrugated profiles", *Bull. Pol. Acad. Sci. Tech. Sci.* 65(6), 791–798 (2017).
- [27] M. Cieszko, R. Drelich, and M. Pakuła, "Wave dispersion in randomly layered materials", *Wave Motion* 64, 52–67 (2016).